



University of Dundee

How members of the human gut microbiota overcome the sulfation problem posed by glycosaminoglycans

Cartmell, Alan; Lowe, Elisabeth C.; Baslé, Arnaud; Firbank, Susan J.; Ndeh, Didier A.; Murray, Heath

Published in:

Proceedings of the National Academy of Sciences of the United States of America

DOI:

[10.1073/pnas.1704367114](https://doi.org/10.1073/pnas.1704367114)

Publication date:

2017

Document Version

Publisher's PDF, also known as Version of record

[Link to publication in Discovery Research Portal](#)

Citation for published version (APA):

Cartmell, A., Lowe, E. C., Baslé, A., Firbank, S. J., Ndeh, D. A., Murray, H., Terrapon, N., Lombard, V., Henrissat, B., Turnbull, J. E., Czjzek, M., Gilbert, H. J., & Bolam, D. N. (2017). How members of the human gut microbiota overcome the sulfation problem posed by glycosaminoglycans. *Proceedings of the National Academy of Sciences of the United States of America*, 114(27), 7037-7042. <https://doi.org/10.1073/pnas.1704367114>

General rights

Copyright and moral rights for the publications made accessible in Discovery Research Portal are retained by the authors and/or other copyright owners and it is a condition of accessing publications that users recognise and abide by the legal requirements associated with these rights.

- Users may download and print one copy of any publication from Discovery Research Portal for the purpose of private study or research.
- You may not further distribute the material or use it for any profit-making activity or commercial gain.
- You may freely distribute the URL identifying the publication in the public portal.

Take down policy

If you believe that this document breaches copyright please contact us providing details, and we will remove access to the work immediately and investigate your claim.



How members of the human gut microbiota overcome the sulfation problem posed by glycosaminoglycans

Alan Cartmell^{a,1}, Elisabeth C. Lowe^{a,1}, Arnaud Baslé^a, Susan J. Firbank^a, Didier A. Ndeh^a, Heath Murray^a, Nicolas Terrapon^b, Vincent Lombard^b, Bernard Henrissat^{b,c,d}, Jeremy E. Turnbull^e, Mirjam Czjzek^{f,g}, Harry J. Gilbert^a, and David N. Bolam^{a,2}

^aInstitute for Cell and Molecular Biosciences, Newcastle University, Newcastle upon Tyne NE2 4HH, United Kingdom; ^bArchitecture et Fonction des Macromolécules Biologiques, CNRS, Aix-Marseille University, F-13288 Marseille, France; ^cInstitut National de la Recherche Agronomique, USC1408 Architecture et Fonction des Macromolécules Biologiques, F-13288 Marseille, France; ^dDepartment of Biological Sciences, King Abdulaziz University, Jeddah 21589, Saudi Arabia; ^eCentre for Glycobiology, Department of Biochemistry, Institute of Integrative Biology, University of Liverpool, Liverpool L69 7ZB, United Kingdom; ^fSorbonne Universités, Université Pierre-et-Marie-Curie, Université Paris 06, F-29688 Roscoff cedex, Bretagne, France; and ^gCNRS, UMR 8227, Integrative Biology of Marine Models, Station Biologique de Roscoff, F-29688 Roscoff cedex, Bretagne, France

Edited by Carolyn R. Bertozzi, Stanford University, Stanford, CA, and approved May 23, 2017 (received for review March 17, 2017)

The human microbiota, which plays an important role in health and disease, uses complex carbohydrates as a major source of nutrients. Utilization hierarchy indicates that the host glycosaminoglycans heparin (Hep) and heparan sulfate (HS) are high-priority carbohydrates for *Bacteroides thetaiotaomicron*, a prominent member of the human microbiota. The sulfation patterns of these glycosaminoglycans are highly variable, which presents a significant enzymatic challenge to the polysaccharide lyases and sulfatases that mediate degradation. It is possible that the bacterium recruits lyases with highly plastic specificities and expresses a repertoire of enzymes that target substructures of the glycosaminoglycans with variable sulfation or that the glycans are desulfated before cleavage by the lyases. To distinguish between these mechanisms, the components of the *B. thetaiotaomicron* Hep/HS degrading apparatus were analyzed. The data showed that the bacterium expressed a single-surface endo-acting lyase that cleaved HS, reflecting its higher molecular weight compared with Hep. Both Hep and HS oligosaccharides imported into the periplasm were degraded by a repertoire of lyases, with each enzyme displaying specificity for substructures within these glycosaminoglycans that display a different degree of sulfation. Furthermore, the crystal structures of a key surface glycan binding protein, which is able to bind both Hep and HS, and periplasmic sulfatases reveal the major specificity determinants for these proteins. The locus described here is highly conserved within the human gut *Bacteroides*, indicating that the model developed is of generic relevance to this important microbial community.

human gut microbiota | glycosaminoglycan degradation | heparin | heparan sulfate | *Bacteroides thetaiotaomicron*

The human colonic microbiota (CM) is crucial to health (1–3). The composition of the CM depends on its ability to access nutrients, which are primarily dietary and host glycans. Dissecting the mechanisms by which complex carbohydrates are used by the CM is critical to understanding the drivers of the ecology of this microbial community and how this process relates to human health.

The major glycan degraders in the CM are the Bacteroidetes (4–6). These organisms access their target polysaccharides through endo-acting enzymes on the bacterial surface followed by import of the oligosaccharides generated, which are depolymerized in the periplasm. The genes encoding these enzyme systems are physically linked into loci termed polysaccharide utilization loci (PULs) (7). A significant proportion of the complex carbohydrates available to the CM is mammalian in origin (4). Despite this knowledge, our understanding of how the CM accesses host/mammalian glycans is fragmentary. Models for the breakdown of high-mannose and complex *N*-glycans by gut *Bacteroides* have been proposed (8), and the ecological significance of removing terminal sialic acid from the epithelial mucosa is established (9). There is, however, a paucity of information on the mechanism by which glycosaminoglycans (GAGs), such as heparin (Hep) and heparan sulfate (HS), are used

by the CM. HS is a major component of the extracellular matrix of mammalian cells and therefore, likely to be available to the gut microbiota via turnover of epithelial cells, whereas Hep is released from mast cells at sites of injury and therefore, may not be as prevalent as HS in the gut (10, 11).

Microbial utilization of Hep and HS poses significant biological challenges. Both glycans differ significantly in their degree of polymerization (DP), which suggests that degradation may occur in different cellular locations, whereas sulfation patterns and the uronic acid (UA) are also variable (Fig. 1) (10). This substantial heterogeneity indicates that either a complex portfolio of enzymes is required to deconstruct these acidic glycans or the enzymes that mediate this process display significant substrate promiscuity. The depolymerization of UA-containing glycans, such as Hep/HS, is mediated by glycoside hydrolases (GHs) and/or polysaccharide lyases (PLs) that are grouped into sequence-based families in the CAZy database (12). Hep/HS are degraded by bacterial PLs belonging to families PL12, -13, and -21. Based on specificity, these PLs can be further broadly grouped into three functional groups,

Significance

The major nutrients available to the human microbiota are complex carbohydrates. Host glycans are important to this microbial community, particularly when dietary carbohydrates are scarce. The host glycans heparin and heparan sulfate are high-priority carbohydrates for *Bacteroides thetaiotaomicron*, a member of the human microbiota. The degradation of these complex carbohydrates is challenging, reflecting their highly variable sulfation patterns. How bacteria have adapted to depolymerize the myriad of substructures of this important class of glycosaminoglycan is unknown. Here, we show how enzyme consortia, displaying complementary functions, target the different features of these host glycans. Structural data reveal that the acidic groups of the glycans are key specificity determinants for enzymes and binding proteins that make up the degradative apparatus.

Author contributions: A.C., E.C.L., H.J.G., and D.N.B. designed research; A.C., E.C.L., A.B., S.J.F., D.A.N., H.M., N.T., V.L., and M.C. performed research; J.E.T. contributed new reagents/analytic tools; A.C., E.C.L., A.B., S.J.F., H.M., N.T., V.L., B.H., M.C., and D.N.B. analyzed data; and A.C., E.C.L., B.H., J.E.T., M.C., H.J.G., and D.N.B. wrote the paper.

The authors declare no conflict of interest.

This article is a PNAS Direct Submission.

Freely available online through the PNAS open access option.

Data deposition: The crystallography, atomic coordinates, and structure factors have been deposited in the Protein Data Bank, www.pdb.org (PDB ID codes 4AK1, 4AK2, 5G2T, 5G2U, and 5G2V).

¹A.C. and E.C.L. contributed equally to this work.

²To whom correspondence should be addressed. Email: david.bolam@ncl.ac.uk.

This article contains supporting information online at www.pnas.org/lookup/suppl/doi:10.1073/pnas.1704367114/-DCSupplemental.

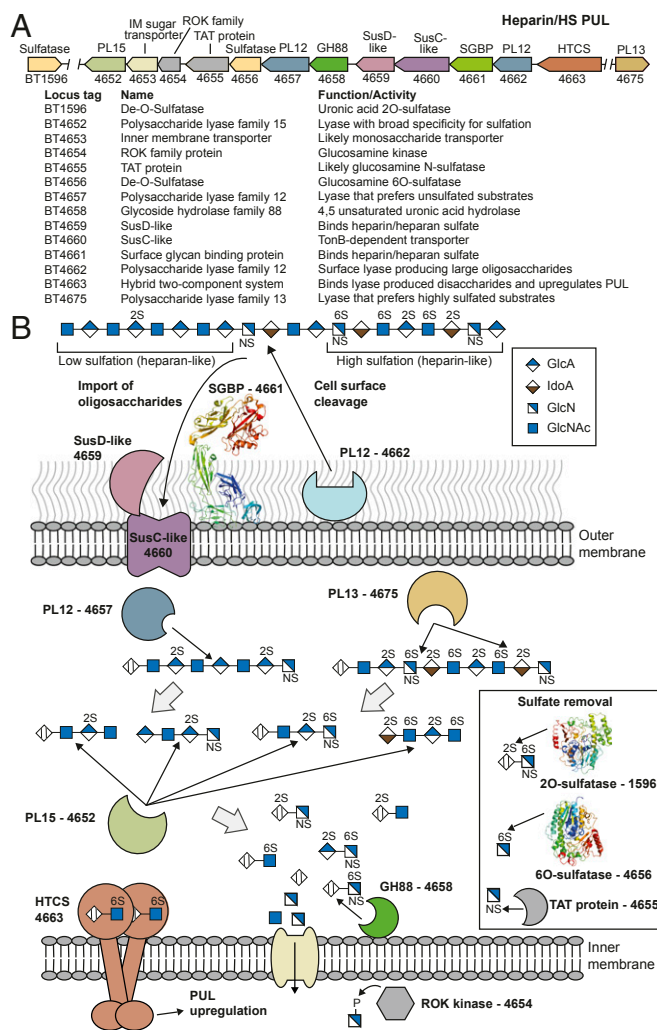


Fig. 1. Model for degradation of Hep and HS by *Bt*. (A) Schematic of the PUL_{Hep} locus in *Bt*. IM, inner membrane. (B) Schematic representation of the cellular location, activity, and specificity of the PUL_{Hep}-encoded enzymes and glycan binding proteins. A typical HS structure is shown. The proteins for which X-ray crystallographic structures were determined in this work are represented by thumbnail images of the structure.

Hep I-III. Hep I lyases require sulfation, Hep II PLs exhibit promiscuity with respect to sulfation patterns, and Hep III enzymes cleave low-sulfation regions of these GAGs (13, 14). The lyases generate products capped by Δ 4,5-unsaturated UA, which is released from the GAG by GHs from family GH88 (13). In addition, some GAG-specific sulfatases have been characterized (15).

Although enzymes active against Hep and HS have been described, how these PLs, GHs, and sulfatases are tailored to act in unison to address the sulfation problem posed by these GAGs is unclear. Several scenarios can be proposed, including desulfation before backbone cleavage, the exploitation of broad specificity PLs that can cleave Hep and HS independent of their sulfation, or the recruitment of a consortium of lyases, with each enzyme targeting specific substructures in these GAGs that differ in their sulfation profiles. Similarly, the mechanisms by which the cell surface glycan binding proteins (SGBPs), which contribute to the glycan degradation machinery, target conserved features of these heterogeneous glycans are unknown.

Bacteroides thetaiotaomicron (*Bt*), a member of the CM, uses Hep and HS as high-priority nutrient sources that activate a single PUL (PUL_{Hep}) (16). Here, we have dissected the mechanism by

which the enzymes and binding proteins encoded by this locus fully deconstruct these highly variable GAGs and thus, solve the sulfation problem. Crystal structures of key proteins provide mechanistic insight into substrate and ligand recognition. The data revealed how the specificity of the apparatus is optimized to target the repertoire of GAG structures presented to the bacterium at the different stages of the degradative process.

Results

Structure of HS and Hep. Hep and HS are composed of a disaccharide repeating unit comprising a UA, D-glucuronic (GlcA), or L-iduronic acid (IdoA) alternating with D-glucosamine (GlcN). GlcN is linked α 1,4 to the UA, whereas IdoA and GlcA are linked α 1,4 and β 1,4, respectively, to the amino sugar (10) (Fig. 1). GlcN can be sulfated on O6 and sulfated or acetylated at N2 (GlcNAc), whereas the UAs are often sulfated on O2. Hep contains significantly more IdoA than HS and is almost completely sulfated, whereas HS varies in its sulfation pattern, containing highly sulfated regions (Hep-like) and areas that contain little or no sulfation (Fig. 1). The DP of Hep (~40) is substantially less than that of HS (~80–200).

PUL_{Hep} Structure. *Bt* grows on Hep, HS, and N-acetyl-de-O-sulfated heparin (Δ SHep) (Fig. S1) (16, 17). Transcriptomics of *Bt* cultured on Hep indicate that only PUL_{Hep}, extending from *bt4652* to *bt4675*, was up-regulated in response to this GAG (16). The locus encodes PLs, sulfatases, a GH88, and a member of the repressor, ORF, kinase (ROK; Pfam PF00480) family (Fig. 1). In addition, the sulfatase BT1596 is also up-regulated by Hep (15). PUL_{Hep} encodes a single SusC/SusD-like outer membrane glycan transporter system and a potential SGBP (Fig. 1). In silico analysis of the occurrence of PUL_{Hep} suggests that it is widely distributed within the *Bacteroides* and retains high sequence conservation and synteny (Fig. S2).

SGBPs. The extracellular location of the putative SGBP, BT4661, was revealed by immunofluorescence and proteinase K treatment using antibodies against the protein (Fig. S3 A and B). Immunoprecipitation of BT4661 from Hep-grown cells followed by Western blotting revealed the presence of BT4659^{SusD-like}, indicating that the two proteins physically associate (Fig. S3C). The interaction between the PUL-encoded SGBP and SusD-like is consistent with previous data from the starch utilization system of *Bt* (18). The importance of BT4659^{SusD-like} in Hep/HS utilization was highlighted by the severe lag (>20 h) displayed by Δ *bt4659*^{SusD-like} on these GAGs (Fig. S14). By contrast, Δ *bt4661*^{SGBP} had no growth defect on Hep-derived oligosaccharides (Fig. S14, Inset). These data suggest that the SGBP plays a role in oligosaccharide scavenging rather than polysaccharide acquisition, such as observed in *Bacteroides ovatus*-mediated xyloglucan degradation (19).

Glycan specificity. Isothermal titration calorimetry (ITC) (Fig. 24 and Table S1) revealed that BT4661^{SGBP} bound tightly to both Hep and HS ($K_d \sim 3 \mu$ M) but did not bind to other GAGs. Notably, coverage on both GAGs was similar, suggesting the protein can tolerate both sulfated and unsulfated regions and could interact or accommodate the different UAs and neutral sugars in Hep and HS (Fig. 1). BT4661^{SGBP} bound to oligosaccharides with a DP ≥ 4 , with affinity increasing up to DP = 6 to a level similar to Hep. These data indicate that the BT4661^{SGBP} binding site can accommodate a hexasaccharide and supports the ability of the SGBP to tolerate/recognize sulfation and IdoA at all subsites (Table S1). These data show that BT4661^{SGBP} is an SGBP of the Hep/HS degrading apparatus and that the protein can accommodate a range of Hep-based GAG structures.

BT4659^{SusD-like} bound Hep, HS, and Δ SHep with similar affinity, but the K_d was ~20- to 30-fold lower than that for the BT4661^{SGBP}. Differences in affinity between the SusD-like and

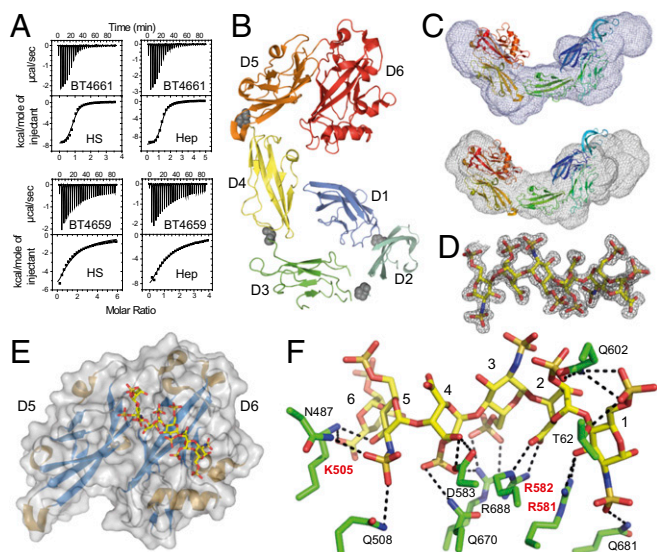


Fig. 2. Structural and biochemical characterization of the PUL_{Hep}-encoded SGBP BT4661. (A) ITC traces for (Upper) BT4661^{SGBP} and (Lower) BT4659^{SusD-like} against HS and Hep. (B) Cartoon representation of BT4661^{SGBP} colored from blue to red from the N terminus to the C terminus. Each of six discrete domains is labeled. Gray spheres show the positions of the interdomain prolines. (C) SAXS envelopes (gray mesh) for (Upper) apoBT4661^{SGBP} and (Lower) BT4661^{SGBP} + Hep. The best fit of the crystal structure of BT4661^{SGBP} (colored from blue to red from the N terminus to the C terminus) is shown inside the SAXS envelopes. (D) 2Fo-Fc map contoured at 1.0 sigma for fully sulfated Hep-derived hexasaccharide in complex with BT4661^{SGBP}. (E) Structure of D5 and D6 C-terminal domains of BT4661^{SGBP} bound to Hep hexasaccharide (carbons as yellow sticks). (F) Ligand binding site of BT4661^{SGBP} bound to fully sulfated Hep hexasaccharide. Amino acid side chains are shown in green, the sugars are in yellow, and H bonds between the ligand and protein are black dotted lines. The residues labeled in red are critical for ligand recognition. The six sugar binding subsites are labeled one to six from the reducing end of the oligosaccharide.

cognate SGBP have been reported previously and may reflect the proposed different roles that these proteins play in glycan utilization (5, 19).

Structure of full-length BT4661^{SGBP}. The crystal structure of BT4661^{SGBP} (Table S2) revealed six discrete domains that adopt an Ig-like fold (Fig. 2B). This multi-Ig-like domain structure is common to the other three SGBPs, which have structures that are known, although little or no sequence identity is evident between these proteins (5, 19, 20). The domains, defined as D1 (N terminus) to D6 (C terminus), are arranged in an extended, curved conformation. Interdomain proline residues may limit the flexibility of the SGBP (19). Small angle X-ray scattering (SAXS) on full-length BT4661^{SGBP} in the presence and absence of Hep gave the same R_g and D_{max} values for both conditions (Table S3), indicating that no large conformational changes are imposed by the target GAG (Fig. 2C, SI Results, and Fig. S3D).

Structure of truncated BT4661^{SGBP} bound to oligosaccharide. Attempts to obtain a ligand complex of full-length BT4661 were unsuccessful. A truncated form of the protein comprising only D5 and D6 displayed similar ligand binding to the WT SGBP. The crystal structure of the D5/6 derivative (TrBT4661^{SGBP}) was determined in complex with a fully sulfated, Hep-derived unsaturated hexasaccharide ($\Delta 4,5\text{UA}2\text{S-GlcNS}6\text{S-IdoA}2\text{S-GlcN}6\text{S-IdoA}2\text{S-GlcNS}6\text{S}$) (Fig. 2D–F and Table S2). The binding site is formed across the D5 and D6 domains, with the reducing end of the hexasaccharide, GlcNS6S, lying in D6 (subsite 1) and the nonreducing end $\Delta\text{UA}2\text{S}$ located in D5 (subsite 6). D6 and D5 house sugars 1–4 and 5 and 6 of the hexasaccharide, respectively. The presence of the glycan binding site on the C-terminal domain of an extended multidomain SGBP has been observed previously and may be an adaptation to

enable ligand binding to occur at a distance from the cell surface (19). Similar to other GAG binding proteins, interactions between ligand and protein mainly involved basic amino acids rather than aromatic residues, which is the characteristic signature of protein–carbohydrate recognition of neutral glycans (10, 19–21). Alanine scanning mutagenesis revealed that K505, R581, and R582 are the key residues involved in ligand binding (Fig. S3E). R582 and K505 interact with the carboxylates of the UA at subsites 2 and 6, respectively, whereas R581 interacts with O3 of the reducing end sugar. These interactions will be conserved in all Hep-based GAGs, providing an explanation for the ability of BT4661 to recognize both HS and Hep with similar affinity.

Enzymes Encoded by PUL_{Hep}. The activity of the PLs sulfatases and GH encoded by PUL_{Hep} was determined against different substrates, and the growth of mutant strains lacking active forms of these enzymes on Hep, HS, and ΔSHep was assessed (Fig. S1B–F). **Surface lyase BT4662^{PL12}.** The lipoprotein BT4662^{PL12} was shown to be a surface enzyme (Fig. S3B) that was active on Hep, ΔSHep , and HS, with a preference for the latter substrate (Fig. 3A and Table S4). Aerobic whole-cell assays, which report only on the activity of surface enzymes, showed that the pattern of reaction products closely matches that of recombinant BT4662^{PL12} (Fig. S4A), confirming the cellular location of the PL. The range of oligosaccharides generated during the early stages of GAG degradation points to an endo-activity (Fig. 3A and Fig. S4E). In other characterized PULs, a surface endo-acting glycanase plays a key role in polysaccharide utilization by generating oligosaccharides that are of an appropriate size to be transported by the SusC/D-like apparatus (5). However, the $\Delta\text{bt}4662^{\text{PL12}}$ *Bt* mutant displayed only a partial growth defect on HS (Fig. S1B), likely reflecting the heterogeneity of the DP of the GAG; thus, the smaller forms of this glycan were able to be transported into the periplasm of *Bt* without the need for prior depolymerization. Growth on Hep and ΔSHep was not impaired in the $\Delta\text{bt}4662^{\text{PL12}}$ mutant, reflecting their low DP, which likely enables these molecules to be transported into the periplasm without prior enzymatic processing.

End point assays revealed that Hep was almost completely inaccessible to BT4662^{PL12} (only ~5% degradation), whereas the depolymerization values of HS and ΔSHep were ~40 and ~80%, respectively (Table S5). Against HS, the limit products comprised a wide range of products, whereas complete degradation of ΔSHep

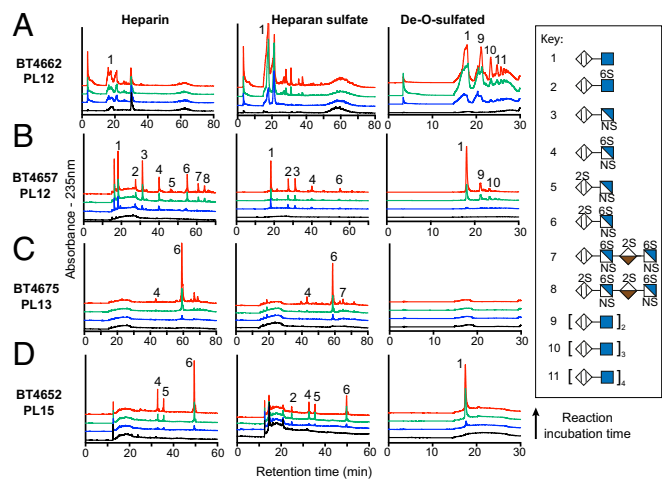


Fig. 3. Product profile of the PUL_{Hep}-encoded PLs against Hep, HS, and ΔSHep . (A) BT4662, (B) BT4657, (C) BT4675, and (D) BT4652. Peaks were identified by comparison with known standards at A_{235} . Black lines represent zero time points, whereas blue, green, and red lines represent early, middle, and late points, respectively, in the reaction time course for each enzyme.

generated oligosaccharides with a DP of 2–10 (Fig. 3A and Fig. S4E). BT4662^{PL12} was only active against Hep oligosaccharides with a DP \geq 10 (Table S4). These data suggest BT4662^{PL12} has a large substrate binding cleft, in which sulfate groups can only be accommodated at specific positions, and the enzyme displays an endo mode of action, with limited processivity. These data are consistent with a role for the enzyme in depolymerizing high molecular weight GAGs, such as HS, at the bacterial surface.

Periplasmic PLs. Based on proteinase K treatment and the product profiles of whole-cell assays compared with those of the recombinant enzymes, the majority of the polysaccharide-degrading enzymes encoded by PUL_{Hep} are located in the periplasm (Figs. S3B and S4A) and display no evidence for metal dependence. A unifying feature of the three periplasmic PLs, BT4652^{PL15}, BT4657^{PL12}, and BT4675^{PL13}, is the appearance of limit disaccharide products during the initial phase of degradation (Fig. 3B–D). This activity is indicative of a degree of processivity and likely results in rapid production of the disaccharides that act as the signaling cue(s) required to up-regulate PUL_{Hep} (17). The three periplasmic lyases have differing preferences for Hep, HS, and Δ SHep (described in detail below), reflecting the ability of *Bt* to use these three substrates.

BT4657^{PL12} exhibited the greatest activity against HS and could access \sim 50% of the polymer; while against Hep, the lyase cleaved 27% of the glycosidic bonds (Tables S4 and S5). The enzyme completely degraded Δ SHep to a single unsulfated disaccharide species (Fig. 3B and Tables S4 and S5). During the initial degradation of Δ SHep, BT4657^{PL12} generated a range of oligosaccharides, with the disaccharide being the dominant product (Fig. 3B and Fig. S4E). These data indicate that BT4657^{PL12} is primarily endo-acting, with a degree of processivity. The products generated from partially sulfated oligosaccharides showed that BT4657^{PL12} is unable to accommodate 2-O sulfation of UA in its active site (+1 subsite), explaining why the enzyme displayed limited activity against Hep (SI Results).

In contrast, BT4675^{PL13} displayed highest activity against Hep and was inactive against Δ SHep, consistent with a previous study suggesting that sulfation was required for activity (Table S4) (22). The requirement for sulfation was mirrored in the end point assays, which showed almost complete digestion of Hep but only \sim 50% of HS (Table S5). The PL13 enzyme generated a range of different size products indicative of an endo mode of action but also displayed significant processivity, because UA2S-GlcNS6S was the dominant product early in the reaction (Fig. 3C).

PL15 enzymes have previously only been shown to be alginate lyases (23). BT4652^{PL15}, however, was active on all three GAGs tested. The enzyme was \sim 800-fold more active against fully sulfated Hep oligosaccharides compared with Δ SHep, indicating that sulfation was key for optimal activity (Table S4), consistent with the production of UA2S-GlcNS6S, UA2S-GlcNS, and UA-GlcNS6S from Hep; however, against HS, an additional disaccharide, UA-GlcNAc6S, was generated, and the unsulfated disaccharide UA-GlcNAc was produced only from Δ SHep (Fig. 3D). BT4652^{PL15} generated disaccharides against all substrates; no intermediate products were observed during initial degradation (Fig. 3D and Fig. S4D). These data indicate the enzyme is exclusively exo-processive and can accommodate sulfates at all positions of the substrate. Although sulfation is not essential, it is a specificity determinant, and as such, BT4652^{PL15} displays more substrate flexibility than BT4675^{PL13}.

The data described above suggest that BT4652^{PL15} and BT4675^{PL13} can target similar heavily *O*-sulfated regions of Hep and HS, although the PL15 enzyme can, in addition, cleave sparsely sulfated regions of these GAGs. Consistent with this view is the observation that mutant strains lacking BT4652^{PL15} or BT4675^{PL13} displayed growth defects on Hep and to a lesser extent, HS but not Δ SHep (Fig. S1B–E). The growth properties of Δ bt4657^{PL12} revealed a significant role for BT4657^{PL12} in HS degradation. The endo-acting lyase likely cleaves areas low in sulfation, creating

nonreducing ends that are targeted by BT4652^{PL15} and BT4675^{PL13}. Our data thus provide a biological context for the multiple lyases expressed by *Bt* in response to Hep and HS (Discussion). The primary substrates for BT4675^{PL13} and BT4657^{PL12} are regions of the GAGs that were highly and poorly sulfated, respectively. The Δ bt4652^{PL15} strain had the largest growth defect on Hep, whereas Δ bt4652^{PL15}/ Δ bt4657^{PL12} displayed little growth on HS and a marked increase in the lag phase when cultured on Δ SHep (Fig. S1D). These growth profiles suggest that BT4657^{PL12} and BT4675^{PL13} produce oligosaccharides that only BT4652^{PL15} can degrade, and thus, the additional flexibility in recognition by the PL15 bridges the two complementary activities of the PL12 and PL13 enzymes (discussed in detail below).

GH88 enzyme. BT4658^{GH88} belongs to a family of enzymes that cleave the glycosidic linkage between the Δ 4,5-unsaturated UA and GlcN/GlcNAc disaccharides that are produced by GAG lyases. The enzyme was not active when O2 of the UA was sulfated but could accommodate sulfation at N2 or O6 of the neutral sugar, mirroring the binding specificity of the PUL_{Hep} hybrid two-component system (HTCS) BT4663 (Table S6) (17). The tuning of the specificity of the GH88 enzyme with that of its cognate HTCS is analogous to that observed in the *Bt* chondroitin sulfate PUL, indicating a conserved role for these enzymes in controlling the rate of signal degradation during growth on GAGs (24). Although BT4658^{GH88} displayed similar catalytic efficiencies against GlcNS and GlcNAc, the K_m and k_{cat} for the sulfated sugar were lower, suggesting that the *N*-linked sulfate contributes to substrate binding but restricts product departure, leading to a reduced k_{cat} .

O-sulfatases. A previous study showed that BT1596^{2S-sulf} and BT4656^{6S-sulf} are exo-acting *O*-sulfatases; BT1596^{2S-sulf} targets the O2 sulfation of unsaturated UA at the nonreducing end of di- and oligosaccharides, whereas BT4656^{6S-sulf} cleaves the O6-sulfate of the monosaccharide GlcNAc6S or GlcNS6S but is inactive against GalNAc6S (Table S6) (15). To explore the mechanism of substrate recognition, the crystal structures of inactive forms of the two *Bt* *O*-sulfatases were determined in complex with their substrates.

BT1596^{2S-sulf} and BT4656^{6S-sulf} share a conserved α/β hydrolase fold comprising a single domain (Fig. 4, Upper and Table S2). Both enzymes have a pocket topology with metal binding sites located at the base of the pocket. Calcium was modeled into the BT4656^{6S-sulf} ligand-bound structure, whereas no metal was observed in BT1596^{2S-sulf} (Fig. 4, Lower). Alanine substitution of the residues in this pocket inactivated both enzymes, revealing the active site location (SI Results and Table S6).

Inactive forms of BT1596^{2S-sulf} and BT4656^{6S-sulf} were cocrySTALLIZED with Δ UA2S-GlcNS6S and GlcNS6S, respectively (Fig. 4). BT1596^{2S-sulf} and BT4656^{6S-sulf} were inactive when expressed in *Escherichia coli*, because the enteric bacterium cannot convert S64 and S77, respectively, into formylglycine, which functions as the catalytic nucleophile [to generate the formylglycine in *E. coli*, the catalytic serine was mutated to cysteine because the bacterium can convert cysteine to formylglycine (25)]. The essential histidines H188 in BT1596^{2S-sulf} and H196 in BT4656^{6S-sulf} are in close proximity to the scissile bond (Fig. 4, Lower and Table S6). Thus, H188 and H196 are ideal candidates for the catalytic acid that is required to protonate the O2/O6 of the departing sugar after nucleophilic attack by the formylglycine and formation of a sulfate-enzyme intermediate, which is then cleaved via a β -elimination to complete the catalytic cycle.

In BT1596^{2S-sulf}, the carboxylate of Δ UA2S makes a bidentate ionic interaction with R237, and loss of this interaction (R237A) results in a 2,000-fold reduction in catalytic efficiency (Fig. 4A and Table S6). This interaction is likely the major specificity determinant used by the enzyme and explains why the sulfatase acts on chondroitin disaccharides, which also possess O2-sulfated UA. In BT4656^{6S-sulf}, R363 and D361 coordinate O4, and mutation of R363 to Ala caused an \sim 500-fold decrease in activity, whereas

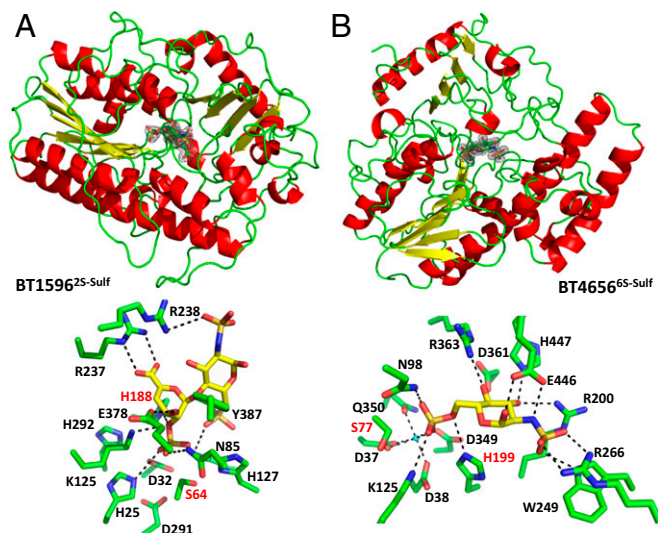


Fig. 4. Sulfatase structures. *Upper* shows cartoon representations of (A) BT1596^{2S-sulf} and (B) BT4656^{6S-sulf}. 2Fo-Fc maps contoured at 1.0 sigma for Δ4,5UA2Sβ1-4GlcNS6S in complex with BT1596^{2S-sulf} and GlcNS6S in complex with BT4656^{6S-sulf} are shown in the respective enzymes active sites. *Lower* shows stick representations of the active site interactions between (A) BT1596^{2S-sulf} and Δ4,5UA2Sβ1-4GlcNS6S and (B) BT4656^{6S-sulf} and GlcNS6S. Amino acid side chains are shown in green, the sugars are in yellow, and H bonds between the sugar and protein are black dotted lines. Residues labeled in red are the key catalytic amino acids.

D361A was inactive (Table S6). These amino acids are likely specificity determinants for gluco- over galacto-configured substrates. (SI Results has a description of all mutants.)

N-sulfatase. There are no predicted sulfamidases in PUL_{Hep}; however, GlcNS does not accumulate during growth on Hep, indicating that *Bt* uses this sugar (Fig. S4F). We deleted the remaining uncharacterized ORF in PUL_{Hep}, *bt4655*. This mutant displayed a growth defect on sulfated GAGs, and GlcNS accumulated in the media during growth on Hep (Figs. S1F and S4F). These data indicate that BT4655 cleaves the sulfamate linkage and is a previously uncharacterized class of sulfatase. Unfortunately, the proposed role of BT4655 as a sulfamidase could not be confirmed biochemically, because a soluble recombinant form of the protein could not be generated.

The data show that the three sulfatases are key for both Hep and HS breakdown. BT1596^{2S-sulf} is the first to act, removing 2-O sulfation from the limit PL-derived disaccharide and allowing BT4658^{GH88} to hydrolyze its target linkage, because this enzyme does not use 2-O-sulfated substrates. The sulfated glucosamine monosaccharides are then substrates for BT4656^{6S-sulf} and the likely sulfamidase BT4655 (Table S6).

Cytoplasmic Sugar Kinase. BT4654^{ROK} is a cytoplasmic member of the ROK protein family that possesses the conserved DxGxT motif and thus, likely an ATP-dependent kinase (26). This activity was confirmed by the capacity of the enzyme to phosphorylate gluco- and manno-configured substrates but not galacto-configured sugars (Table S6). The k_{cat}/K_m of the enzyme decreased from GlcN > GlcNAc >> Glc/Man >> GlcNS, which was driven by increases in K_m (Table S6). These data show that O4 is critical for catalysis, whereas strong selection in affinity is made at C2 for an equatorial amine, indicating that BT4654^{ROK} uses both an equatorial N2 and an O4 as specificity determinants. Because the Δ*bt4654*^{ROK} mutant displayed no growth defect on Hep or HS (Fig. S1F), *Bt* seems to display redundancy in GlcN and GlcNAc phosphorylation.

Discussion

Bt PUL_{Hep} orchestrates the hierarchical degradation of Hep and HS. Both of these GAGs could be derived from dietary meat or host glycans. In vivo expression of PUL_{Hep} in mice colonized with *Bt* has only been observed in bacteria occupying the mucosal layer, suggesting that the source of Hep/HS available to *Bt* is from the turnover of epithelial cells rather than the diet (27). HS could also be supplied in the human diet as a component of meat; however, colonic metagenomic data obtained in a study, which swapped subjects from vegetarian diets to meat-rich diets, did not reveal any PL families associated with the degradation of Hep/HS (28). These data support the hypothesis that the source of Hep/HS in the human gut accessible to the microbiota is from the turnover of epithelial cells. Goodman et al. (29) identified through transposon mutagenesis genes in *Bt* important for colonization of the mouse gut. Strains with insertions in the *bt4659*^{stusD-like} were significantly decreased in the output from the monocolonized mouse gut compared with input. Interestingly, in mice cocolonized with six other Bacteroidetes strains in addition to the *Bt* mutant population, *bt4658*^{GH88} and *bt4661*^{SGBP} insertion mutants were much lower in abundance than in monocolonized mice, indicating that the ability to degrade HS is under increased selection pressure for *Bt* in the presence of other Bacteroidetes (Fig. S2).

Within the Hep-based GAGs, there is substantial structural diversity, especially in terms of the level of sulfation, and it is this heterogeneity that provides an explanation for the distinct but complementary activities of the enzymes encoded by the PUL_{Hep}. A key feature of the PUL_{Hep} degradative apparatus is the surface lyase, BT4662^{PL12}, which although dispensable for growth on Hep, plays a significant role in optimal HS utilization. This difference likely reflects the high DP of HS relative to Hep, and thus, the GAG needs to be subjected to a degree of extracellular depolymerization to generate molecules that can be imported into the periplasm (5).

In the periplasm, the substrate specificity of endoprocessive lyases is optimized to target highly sulfated (BT4675^{PL13}) or low/unsulfated regions (BT4657^{PL12}), producing small oligosaccharides that only the exoprocessive lyase (BT4652^{PL15}) is able to degrade. This role for BT4652^{PL15} is critical, because loss of the enzyme means that elements of both Hep and HS remain inaccessible to *Bt*. The presence of a PL15 lyase is a conserved feature of Hep/HS utilization in other Bacteroidetes, supporting its key role in breakdown of these GAGs (Fig. S2). The synergistic specificities displayed by the PUL_{Hep} lyases enable the bacterium to cleave the backbone of GAGs that display substantial structural variation, particularly in their sulfation patterns, leading to the generation of disaccharides. The disaccharides are broken down by the complementary activities of the sulfatases and the GH88 enzyme-generating sugars that can then be metabolized by the bacterium.

Bt places a high priority on Hep and HS utilization shown by the lack of repression of PUL_{Hep} by other polysaccharides and glucose (30). HS is an abundant source of GlcNAc, which is required for the synthesis of peptidoglycan. Although *Bt* seems to contain all of the biosynthetic genes needed to make GlcNAc, it may still prioritize GlcNAc derived from glycans to synthesize its cell wall. As stated above, we propose that *Bt* uses HS/Hep from the host mucosa rather than the diet. Because the epithelium is likely to contain much higher amounts of HS compared with Hep, we believe that the biologically relevant glycan targeted by PUL_{Hep} is HS. Analysis of the genomes of other members of the CM revealed PULs similar to *Bt* PUL_{Hep} (Fig. S2). *Bacteroides xylanisolvens* and *Bacteroides ovatus* both contain a predicted surface PL12 lyase similar to BT4662^{PL12}, suggesting that these organisms also target HS. In contrast, the GAG-degrading apparatus of *Bacteroides intestinalis* lacks an obvious surface Hep/HS lyase (Fig. S2). Thus, the bacterium may target oligosaccharides or low molecular weight

GAGs, such as Hep, which can be imported without the need for enzymatic depolymerization.

The structural data of the sulfatases showed that the interactions with the target sulfate are highly conserved in BT1596^{2S-sulf}, BT4656^{6S-sulf}, and the human 6S GalNAc sulfatase (GALNSase) (Fig. S3F). In BT4656^{6S-sulf} and GALNSase (the only other 6-O carbohydrate sulfatase for which a structure is available; Protein Data Bank ID code 4FDI), however, there is very little conservation in the residues that interact with the carbohydrate component of the substrate (Fig. S3G), showing that this area is highly variable and could be the basis for bespoke highly specific glycosulfatase inhibitors. Such inhibitors may have therapeutic relevance, because a recent study showed that, in a colitis-sensitive mouse model, sulfatases expressed by *Bt* are essential factors in inducing the disease (31).

Conclusions

This report describes the characterization of a PUL that orchestrates the degradation of Hep/HS, high-priority heterogeneous glycans. Unlike other microbial systems that remove side chains before backbone degradation, the glycan backbone of Hep/HS is depolymerized before removal of the sulfate groups. To achieve this depolymerization, *Bt* expresses lyases with complementary activities that, in combination, can fully deconstruct the Hep-based GAGs. The PLs, sulfatases, and GH encoded by PUL_{Hep} provide an example of how an enzyme consortium can degrade substrates that display highly variable sulfation patterns. Understanding the

mechanisms by which gut bacteria depolymerize GAGs may provide crucial insights into how the human gut microbiota is adapted to use nonmucin host glycans and the role that this process plays in colonization and survival in the gut. The model developed here can be harnessed to interrogate metagenomic data to explore the mechanisms by which different members of the microbiota metabolize these complex GAGs.

Materials and Methods

Bacteroides Culture and Genetic Manipulation. *Bt* VPI-5482 was cultured anaerobically, and genomic null mutations were generated as described previously (16, 32).

Enzyme Assays. PL activity was monitored at A₂₃₅. BT4658^{GH88} glucuronyl hydrolase activity was determined by monitoring loss of signal at A₂₃₅. Sulfatase and kinase activities were determined through either linked assays or HPLC. Products were analyzed by TLC and/or HPLC.

Crystallization of BT1596, BT4656, and BT4661. Crystallization and structure determination were as described in *SI Materials and Methods*.

Full details of all experimental procedures used are described in *SI Materials and Methods*.

ACKNOWLEDGMENTS. We thank Carl Morland for expert technical assistance. This work was funded by the United Kingdom Biotechnology and Biological Sciences Research Council (Grant BB/F014163/1), the European Research Council (Grant 322820), and the Wellcome Trust (Grant WT097907MA).

- Kau AL, Ahern PP, Griffin NW, Goodman AL, Gordon JI (2011) Human nutrition, the gut microbiome and the immune system. *Nature* 474:327–336.
- Round JL, Mazmanian SK (2009) The gut microbiota shapes intestinal immune responses during health and disease. *Nat Rev Immunol* 9:313–323.
- Bäckhed F, Ley RE, Sonnenburg JL, Peterson DA, Gordon JI (2005) Host-bacterial mutualism in the human intestine. *Science* 307:1915–1920.
- Koropatkin NM, Cameron EA, Martens EC (2012) How glycan metabolism shapes the human gut microbiota. *Nat Rev Microbiol* 10:323–335.
- Rogowski A, et al. (2015) Glycan complexity dictates microbial resource allocation in the large intestine. *Nat Commun* 6:7481.
- Ndeh D, et al. (2017) Complex pectin metabolism by gut bacteria reveals novel catalytic functions. *Nature* 544:65–70.
- Martens EC, Koropatkin NM, Smith TJ, Gordon JI (2009) Complex glycan catabolism by the human gut microbiota: The Bacteroidetes Sus-like paradigm. *J Biol Chem* 284:24673–24677.
- Cao Y, Rocha ER, Smith CJ (2014) Efficient utilization of complex N-linked glycans is a selective advantage for *Bacteroides fragilis* in extraintestinal infections. *Proc Natl Acad Sci USA* 111:12901–12906.
- Tailford LE, et al. (2015) Discovery of intramolecular trans-sialidases in human gut microbiota suggests novel mechanisms of mucosal adaptation. *Nat Commun* 6:7624.
- Gandhi NS, Mancera RL (2008) The structure of glycosaminoglycans and their interactions with proteins. *Chem Biol Drug Des* 72:455–482.
- Oshiro M, et al. (2001) Immunohistochemical localization of heparan sulfate proteoglycan in human gastrointestinal tract. *Histochem Cell Biol* 115:373–380.
- Lombard V, et al. (2010) A hierarchical classification of polysaccharide lyases for glyco-genomics. *Biochem J* 432:437–444.
- Nakamichi Y, Mikami B, Murata K, Hashimoto W (2014) Crystal structure of a bacterial unsaturated glucuronyl hydrolase with specificity for heparin. *J Biol Chem* 289:4787–4797.
- Ulaganathan T, et al. (2017) Conformational flexibility of PL12 family heparinases: Structure and substrate specificity of heparinase III from *Bacteroides thetaiotaomicron* (BT4657). *Glycobiology* 27:176–187.
- Ulmer JE, et al. (2014) Characterization of glycosaminoglycan (GAG) sulfatases from the human gut symbiont *Bacteroides thetaiotaomicron* reveals the first GAG-specific bacterial endosulfatase. *J Biol Chem* 289:24289–24303.
- Martens EC, Chiang HC, Gordon JI (2008) Mucosal glycan foraging enhances fitness and transmission of a saccharolytic human gut bacterial symbiont. *Cell Host Microbe* 4:447–457.
- Lowe EC, Baslé A, Czjzek M, Firbank SJ, Bolam DN (2012) A scissor blade-like closing mechanism implicated in transmembrane signaling in a *Bacteroides* hybrid two-component system. *Proc Natl Acad Sci USA* 109:7298–7303.
- Cho KH, Salyers AA (2001) Biochemical analysis of interactions between outer membrane proteins that contribute to starch utilization by *Bacteroides thetaiotaomicron*. *J Bacteriol* 183:7224–7230.
- Tauzin AS, et al. (2016) Molecular dissection of xyloglucan recognition in a prominent human gut symbiont. *MBio* 7:e02134–e15.
- Cameron EA, et al. (2012) Multidomain carbohydrate-binding proteins involved in *Bacteroides thetaiotaomicron* starch metabolism. *J Biol Chem* 287:34614–34625.
- Boraston AB, Bolam DN, Gilbert HJ, Davies GJ (2004) Carbohydrate-binding modules: Fine-tuning polysaccharide recognition. *Biochem J* 382:769–781.
- Han YH, et al. (2009) Structural snapshots of heparin depolymerization by heparin lyase I. *J Biol Chem* 284:34019–34027.
- Ochiai A, Yamasaki M, Mikami B, Hashimoto W, Murata K (2010) Crystal structure of exotype alginate lyase Atu3025 from *Agrobacterium tumefaciens*. *J Biol Chem* 285:24519–24528.
- Raghavan V, Lowe EC, Townsend GE, 2nd, Bolam DN, Groisman EA (2014) Tuning transcription of nutrient utilization genes to catabolic rate promotes growth in a gut bacterium. *Mol Microbiol* 93:1010–1025.
- Dierks T, et al. (1998) Posttranslational formation of formylglycine in prokaryotic sulfatases by modification of either cysteine or serine. *J Biol Chem* 273:25560–25564.
- Titgemeyer F, Reizer J, Reizer A, Saier MH, Jr (1994) Evolutionary relationships between sugar kinases and transcriptional repressors in bacteria. *Microbiology* 140:2349–2354.
- Li H, et al. (2015) The outer mucus layer hosts a distinct intestinal microbial niche. *Nat Commun* 6:8292.
- David LA, et al. (2014) Diet rapidly and reproducibly alters the human gut microbiome. *Nature* 505:559–563.
- Goodman AL, et al. (2009) Identifying genetic determinants needed to establish a human gut symbiont in its habitat. *Cell Host Microbe* 6:279–289.
- Rogers TE, et al. (2013) Dynamic responses of *Bacteroides thetaiotaomicron* during growth on glycan mixtures. *Mol Microbiol* 88:876–890.
- Hickey CA, et al. (2015) Colitogenic *Bacteroides thetaiotaomicron* antigens access host immune cells in a sulfatase-dependent manner via outer membrane vesicles. *Cell Host Microbe* 17:672–680.
- Koropatkin NM, Martens EC, Gordon JI, Smith TJ (2008) Starch catabolism by a prominent human gut symbiont is directed by the recognition of amylose helices. *Structure* 16:1105–1115.
- Reith J, Berking A, Mayer C (2011) Characterization of an N-acetylmuramic acid/N-acetylglucosamine kinase of *Clostridium acetobutylicum*. *J Bacteriol* 193:5386–5392.
- Winn MD, et al. (2011) Overview of the CCP4 suite and current developments. *Acta Crystallogr D Biol Crystallogr* 67:235–242.
- Terrapon N, Lombard V, Gilbert HJ, Henrissat B (2015) Automatic prediction of polysaccharide utilization loci in Bacteroidetes species. *Bioinformatics* 31:647–655.
- Terrapon N, Weiner J, Grath S, Moore AD, Bornberg-Bauer E (2014) Rapid similarity search of proteins using alignments of domain arrangements. *Bioinformatics* 30:274–281.
- Guinier A, Fournet F (1955) *Small Angle Scattering of X-Rays* (Wiley Interscience, New York).
- Svergun D (1992) Determination of the regularization parameter in indirect-transform methods using perceptual criteria. *J Appl Crystallogr* 25:495–503.
- Svergun DI, Petoukhov MV, Koch MH (2001) Determination of domain structure of proteins from X-ray solution scattering. *Biophys J* 80:2946–2953.
- Petoukhov MV, Eady NA, Brown KA, Svergun DI (2002) Addition of missing loops and domains to protein models by x-ray solution scattering. *Biophys J* 83:3113–3125.
- Volkov VV, Svergun DI (2003) Uniqueness of ab initio shape determination in small-angle scattering. *J Appl Crystallogr* 36:860–864.
- Davies GJ, Wilson KS, Henrissat B (1997) Nomenclature for sugar-binding subsites in glycosyl hydrolases. *Biochem J* 321:557–559.